formation of PSt–PMMA block copolymer according to the proposed mechanism. The major ultraviolet absorption at high molecular weight arises almost exclusively from the low molecular weight Br–PSt used as initiator. The elution volumes at which this PSt appears cover the same range as those for elution of the PMMA, consistent with the PSt being present as end-blocks of PSt–PMMA block copolymer. In addition, the two chromatograms are not identical in shape. The peak of the u.v. trace appears at greater elution volume than the peak of the i.r. trace. This result is entirely consistent with block copolymer formation because every PMMA chain will be attached to a PSt block of molecular weight 2000. Therefore, low molecular weight copolymer molecules will contain larger proportions of PSt than the high molecular weight molecules and, hence, will give relatively large u.v. responses, as observed.

Conclusion

The combination of kinetic and molecular weight data presented above establishes that Br–PSt can be used as a source of free radicals capable of initiating the polymerization of MMA leading to the formation of PSt/PMMA block copolymers. Therefore we conclude that we have established an additional route for block copolymer formation by effecting a transformation from anionic propagation (used in the synthesis of PSt) to free-radical propagation through the intermediate formation of Br–PSt.

We are now attempting to determine the potential efficiency of the transformation and to extend the synthesis to other monomer combinations.

Acknowledgement

The authors wish to thank the Ministry of Defence for financial support for J.W. and S.R.C. for funds to purchase the gel permeation chromatograph.

References

1 Richards, D. H. *Br. Polym. J.* 1980, **12**, 89
2 For summary see: Bamford, C. H., in 'Reactivity, Mechanisms and Structure in Polymer Chemistry', (Eds. A. D. Jenkins and A. Ledwith), Wiley, N.Y., 1974, p. 52; Bamford, C. H. *Eur. Polym. J. Suppl.* 1969, p. 1
3 For summary see: Eastmond, G. C. *Pure Appl. Chem.* 1981, **53**, 657
4 Burgess, F. J., Cunliffe, A. V., MacCallum, J. R. and Richards, D. H. *Polymer* 1977, **18**, 719
5 Eastmond, G. C. in 'Free Radical Polymerization', Vol. 14A of Comprehensive Chemical Kinetics, (Eds. C. F. H. Tipper and C. H. Bamford), Elsevier, Amsterdam, 1976, p. 1

Quantitative characterization of orientation in PET fibres by Raman spectroscopy

D. I. Bower and I. M. Ward
Department of Physics, The University of Leeds, Leeds LS2 9JT, UK
(*Received* 12 *November* 1981)

Attempts to obtain quantitative measures of orientation on fibres of diameter $\sim 10\,\mu$m by the method used earlier on films were unsuccessful. This is believed to be due to polarization scrambling caused by reflection and refraction at the surface of the fibre. It is shown that by immersing the fibres in a liquid of refractive index equal to the mean of those of the fibre the method can be used successfully.

Keywords Orientation; fibre; Raman; polymer; spectra; poly(ethylene terephthalate)

Introduction

Raman spectroscopy has been used to characterize quantitatively the degree of molecular orientation in oriented samples of a number of different polymers[1-5] including poly(ethylene terephthalate) (PET). In the studies on uniacially oriented PET, quantitative agreement was found between values of $\langle\cos^2\theta\rangle$, or $\langle P_2(\cos\theta)\rangle$, determined from refractive index measurements and from Raman measurements, where θ is the angle between the chain axis and the draw direction, $P_2(\cos\theta)=\frac{1}{2}(3\cos^2\theta-1)$ and the angle brackets denote the average value. The results of more recent Raman studies of orientation on a biaxially oriented sheet[6] were also consistent with measurements of refractive index.

In all these studies the samples were at least 30 μm thick, and of much greater size in the two directions perpendicular to the thickness, and the propagation directions of both the incident and the analysed Raman scattered light were to a good approximation normal to the edge or to one of the surfaces of the sample. When an attempt was made to apply the method to single-filament yarns of PET of approximate diameter 10 μm, it was found that the values of $\langle P_2(\cos\theta)\rangle$ obtained were very different from those deduced from the birefringence of the fibres. No quantitative explanation has been found so far for the discrepancy, but it is believed that it arises because the incident and Raman scattered light are multiply reflected at the surface of the sample and also refracted on entering or leaving the sample so that their polarization directions become ill-defined when in the plane normal to the fibre axis. The present communication shows that if the fibre is immersed in a liquid with a refractive index close to that of the polymer the discrepancy disappears and meaningful values of both $\langle P_2(\cos\theta)\rangle$ and $\langle P_4(\cos\theta)\rangle$ can be found, where $P_4(\cos\theta)=\frac{1}{8}(3-30\cos^2\theta+35\cos^4\theta)$. In the remainder of this communication we shall abbreviate $\langle P_l(\cos\theta)\rangle$ by P_l.

0032-3861/82/050645-05$03.00

Experimental details

Four samples of heat-set single-filament yarns were studied. The birefringences Δn of the yarns were determined using a Berek compensator and are given in *Table 1*.

Raman spectra of each sample immersed in various liquids were obtained using 90° scattering geometry with the fibre axis (Ox_3) perpendicular to the plane defined by the incident laser beam (Ox_1) and the direction in which the scattered light was observed (Ox_2). The laser beam could be polarized parallel to Ox_3 or Ox_2 and the analyser could be set to transmit light polarized parallel to Ox_3 or Ox_1. For each sample and immersion liquid four spectra were obtained in the region of the strong vibration at $\Delta\tilde{\nu} = 1616\,\text{cm}^{-1}$. They may be designated S_{33}, S_{13}, S_{32} and S_{12} where S_{ij} is the spectrum obtained when the laser beam is polarized parallel to Ox_j and the analyser polarization direction is parallel to Ox_i. Spectra were obtained for all samples immersed in air, water and liquid paraffin. For the sample of highest birefringence, spectra were also obtained with the sample immersed in heptane, dodecane and diiodomethane. The refractive indices of the liquids are given in *Table 1*. For all spectra the laser beam was focussed on the sample by means of a lens of focal length 15 cm. For each of the liquids, spectra corresponding to S_{ij} were obtained under the same conditions, by simply displacing the samples out of the laser beam.

Results and data analysis

The spectra of none of the liquids except diiodomethane show any sharp peaks in the region of the strong 1616 cm^{-1} line of PET and it was therefore possible to measure the intensity I_{ij} of this peak from the corresponding spectrum S_{ij} by drawing in by hand on a chart record of the spectrum a background whose smooth shape was estimated by comparison with the corresponding spectrum of the liquid alone. The peak height above this background was then measured. *Figure 1* shows the spectra S_{33} and S_{12} of the most highly oriented sample in air and in diiodomethane and of diiodomethane alone. It is clear that it is impossible to determine the intensity of the 1616 cm^{-1} line of the sample accurately, particularly for the spectrum S_{12}, by estimating a base line because of the broad peak of the diiodomethane spectrum centred at about 1605 cm^{-1}. The four spectra S_{33}, S_{13}, S_{32} and S_{12} for the sample immersed in diiodomethane were therefore recorded

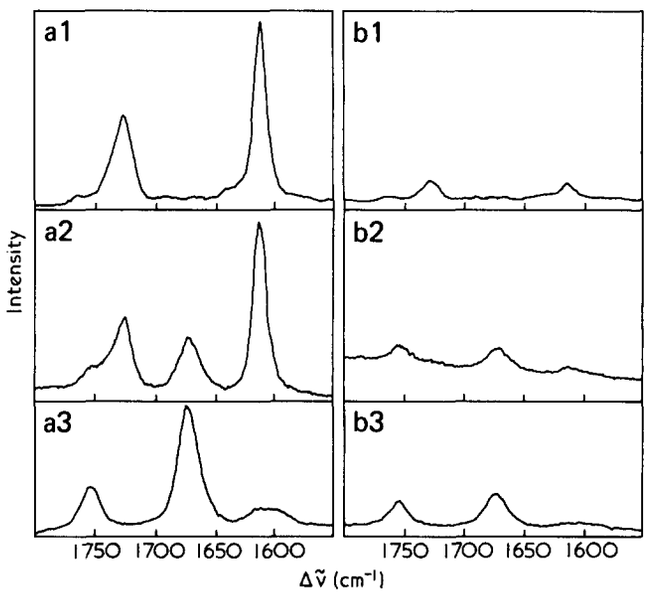

Figure 1 (a) Spectrum S_{33}: a1, sample d in air; a2, sample d in diiodomethane; a3, diiodomethane. (b) Spectrum S_{12}: b1, sample d in air; b2, sample d in diiodomethane; b3, diiodomethane

Table 1 Raman intensity ratios for various immersion liquids

	Sample a	Sample b	Sample c	Sample d
Δn	0.134	0.146	0.169	0.193
Air $n = 1.000$				
R_1	0.621	0.586	0.415	0.228 ± 0.009
R_2	0.454	0.404	0.248	0.084 ± 0.006
Water $n = 1.333$				
R_1	0.247	0.269	0.227	0.136
R_2	0.149	0.145	0.097	0.047
Heptane $n = 1.385$				
R_1				0.139 ± 0.009
R_2				0.037 ± 0.008
Dodecane $n = 1.421$				
R_1				0.136
R_2				0.035
Liquid paraffin $n = 1.483$				
R_1	0.264 ± 0.011	0.252	0.174	0.122
R_2	0.114 ± 0.004	0.120	0.076	0.032
Diiodomethane $n = 1.738$				
R_1				0.112 ± 0.004
R_2				0.032 ± 0.003
Fit				
R_{10}	0.209 ± 0.034	0.216 ± 0.018	0.167 ± 0.005	0.117 ± 0.006
R_{20}	0.087 ± 0.010	0.095 ± 0.010	0.063 ± 0.004	0.030 ± 0.002

digitally on paper tape at intervals of 1 cm^{-1} over the range 1550–1800 cm^{-1}. Similar digital recordings were made of the corresponding spectra of diiodomethane and of the sample in air. Each spectrum of the sample in diiodomethane was then computer fitted by a 'least squares' procedure to a linear background plus a weighted sum of the spectra S_{33}, S_{13} and S_{12} of the sample in air and the spectra S_{33} and S_{13} of diiodomethane, with the weighting factors as the variables in the fit. The total contribution of the background plus the two diiodomethane spectra to the fit was then subtracted from the original spectrum and the resultant spectrum was considered to be that of the sample free from contributions by the liquid. This was plotted out by the computer and a background was drawn and the peak height measured directly from the plot.

The intensity I_{33}, which was always the largest, was taken as standard and the other three spectra were then corrected for the slight difference in intensity of the laser beam for the two polarization directions and for the differential polarization sensitivity of the spectrometer. These corrections were always less than 7%. The mean ratios of the corrected intensities I_{32} and I_{13} for 26 sets was 1.06 with a standard deviation of 0.02. The reason for this small systematic difference is not understood, but it may be due to a different effective polarization scrambling of the incident laser light from that of the emerging Raman-scattered light. The movement of the laser beam when the polarization rotator was rotated has been measured to be less than 5μm and since the diameter of the fibre was ~ 10 μm and that of the diffraction limited focussed laser beam ~ 40 μm, this small movement of the beam is unlikely to be responsible for the difference. In calculating the orientation parameters the mean value of I_{32} and I_{13} was used, and this value is denoted by $\bar{I}_{32}$. The values of $\bar{I}_{32}/I_{33} = R_1$ and $I_{12}/I_{33} = R_2$ are given in *Table 1* and plotted in *Figure 2* and a strong dependence of the intensity ratios on the refractive index of the immersion liquid, especially for the samples of lower orientation, is apparent.

It is believed that the correct ratios would be observed if the refractive index of the immersion liquid was equal to that of the polymer, so that no refraction or reflection of incident or scattered light took place. This equality cannot be satisfied for both incident and scattered light when they have different polarizations because of the birefringence of the sample. If, however, the refractive index of the liquid was equal to $(n_1 + n_3)/2$, where n_3 and n_1 are the refractive indices of the sample for light with polarization vector parallel and perpendicular to the fibre axis, respectively, the residual effects should be very small. An attempt has therefore been made to estimate the values of the intensity ratios for a liquid with this mean refractive index from the observed ratios. Since it is the difference in refractive index between the sample and the liquid which is responsible for the polarization scrambling which produces higher ratios than the 'correct' values, the estimate has been made by assuming a simple parabolic dependence of the intensity ratios on the refractive index of the liquid. The observed intensity ratios have been 'least squares' fitted to parabolae with the general form

$$R - R_0 = a(n - n_0)^2 \qquad (1)$$

where $R = R_1$ or R_2 and $R_0 = R_{10}$ or R_{20}, the required ratio when the refractive index of the liquid is n_0. The fitted parabolae are shown in *Figure 2*.

The fixed values of n_0 for each sample were estimated by using the birefringence of the sample and the data of Nobbs *et al.* for the values of n_3 and n_1 for a series of uniaxially oriented PET tapes[7]. A plot of n_3 or n_1 against $\Delta n = (n_3 - n_1)$ is a very good straight line which enables n_3 and n_1 and hence $(n_3 + n_1)/2$ to be estimated accurately from Δn. The values obtained for the four samples ranged from 1.611 to 1.624 and are shown as bars on *Figure 2*. It should be noted that the lowest and highest refractive indices for the four samples were 1.544 and 1.720, so that the range of indices is small compared with that of the 'liquids' (including air) used and that the parabolae are very flat in this range. The fits were made without any weighting of the results for those liquids where more than one determination had been made for a given sample and the results for R_{10} and R_{20} are shown in the last column of *Table 1*. The uncertainty shown there is the r.m.s. deviation of the points from the parabolae. It should be noted that for the two samples of lower orientation these uncertainties are somewhat larger than, but of the same order as, those estimated from repeated measurements on a given sample.

It follows from equations given by Bower[8] that

$$P_2 = (a_{11}R_1 + a_{12}R_2 + a_{13})/N \qquad (2a)$$

$$P_4 = (a_{21}R_1 + a_{22}R_2 + a_{23})/N \qquad (2b)$$

where

$$N = (a_{31}R_1 + a_{32}R_2 + a_{33}) \qquad (3)$$

and

$$\begin{pmatrix} a_{11} & a_{12} & a_{13} \\ a_{21} & a_{22} & a_{23} \\ a_{31} & a_{32} & a_{33} \end{pmatrix} = \begin{pmatrix} -0.0237 & 0.0587 & -0.0192 \\ 0.1178 & -0.0611 & -0.0311 \\ -0.0548 & -0.0898 & -0.0162 \end{pmatrix}$$

Figure 3 shows families of lines which relate P_4 and P_2 for fixed values of R_1 or R_2. The lines which are nearly

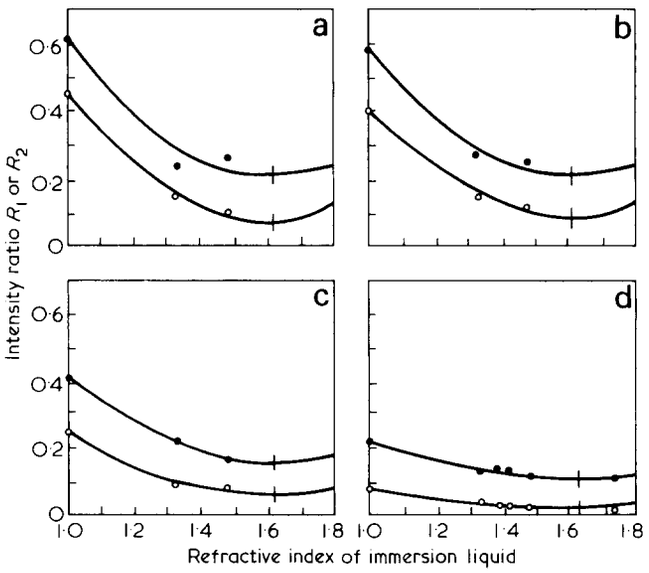

Figure 2 Raman intensity ratios plotted against refractive index of immersion liquid. ●, $\bar{I}_{32}/I_{33} = R_1$; ○, $I_{12}/I_{33} = R_2$; |, 'mean' refractive index of sample

parallel to the P_2 axis in the region of positive values of P_2 and P_4 are for constant R_1 and the lines which are almost normal to them are for constant R_2. Thus, in this positive region, the value of P_2 calculated from equations (2)–(4) depends strongly on R_2 and weakly on R_1, whereas the reverse applies to P_4. Pairs of values of P_2 and P_4 which lie outside the region bounded by the upper straight line and the lower parabola are impossible on purely mathematical grounds for a distribution of orientations in which the number of units at a given orientation is always positive or zero. The figure enables approximate values of P_2 and P_4 to be read off for given values of R_1 and R_2, before using equations (2)–(4) to obtain more precise values.

The numerical values for the a_{ij} were calculated on the following assumptions:

(1) The ratios of the principal components α_1, α_2, α_3 of the Raman tensor for the 1616 cm^{-1} mode are $-0.18:-0.18:1$ (see reference 1).

(2) The principal axis corresponding to α_3 is parallel to the projection of the C_1–C_4 direction onto the mean plane of the *para*-disubstituted benzene ring (see reference 1).

(3) All chains in the sample have locally the same conformation as those in the PET crystal so that, from the data of Daubeny *et al.*[9], the angle between the C_1–C_4 direction and the chain axis is 18° 59′.

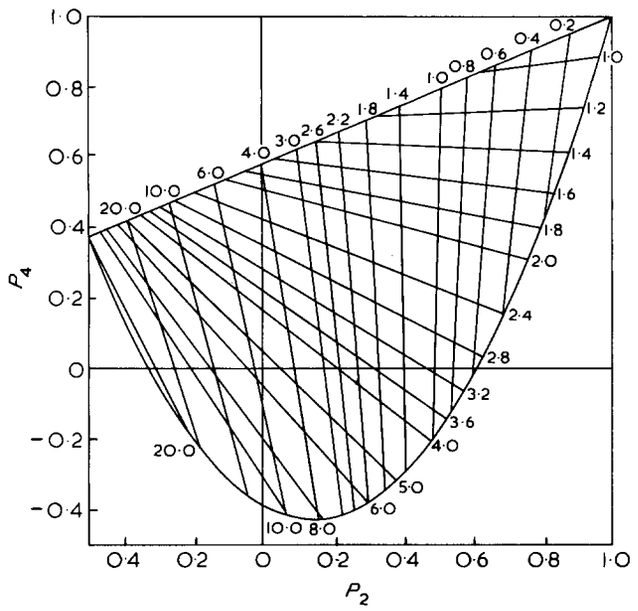

Figure 3 Relationship between P_4 and P_2 for fixed values of R_1 (lines which are nearly parallel to P_2 axis for large P_2 and P_4) and for fixed values of R_2. The constant values of R_1 (multiplied by 10) are given below the lower limit parabola for P_4 and the constant values of R_2 (multiplied by 10) are given above the straight-line upper limit

Table 2 shows the values of P_2 and P_4 calculated using the values of R_{10} and R_{20} and also the value calculated using the ratios R_1 and R_2 determined with the sample in air. For comparison, values of P_2 deduced from the birefringence of the fibres on the assumption that the maximum birefringence is 0.23 ± 0.01 are also shown. It is clear that agreement between the Raman values and the birefringence values is quite good provided that R_{10} and R_{20} are used to calculate the Raman values. If R_1 and R_2 determined with the sample in air are used, the agreement is very poor.

It is not easy to check the values of P_4, but *Figure 4* shows that the relationship between P_4 and P_2 is similar to that obtained earlier by Raman spectroscopy for a series of uniaxially oriented PET tapes[1,2].

Where high accuracy in the determination of P_2 and P_4 is not required it may be sufficient to determine the values of R_1 and R_2 in air and liquid paraffin and to deduce R_{10} and R_{20} from a parabola passing through these points and having its minimum at the mean refractive index of the fibre. The results of this procedure applied to the present data are shown in the last two columns of *Table 2*.

Conclusions

Raman spectroscopy can be used to determine the values of P_2 and P_4 for fibres as well as sheets or tapes, but precautions must be taken that true intensity ratios are obtained. The effective polarization scrambling which

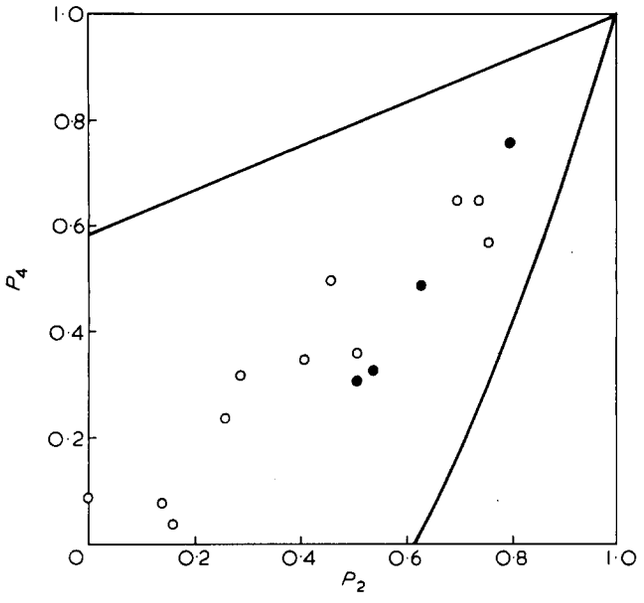

Figure 4 P_4 plotted against P_2. ○, from *Table 2*, reference 2; ●, present results. The lines represent the upper and lower limits on P_4 for a given P_2

Table 2 Orientation averages, P_2 and P_4

		Raman from parabolic fit		Raman from measurements in air		Raman from measurements in air and liquid paraffin	
Sample	Optical P_2	P_2	P_4	P_2	P_4	P_2	P_4
a	0.58 ± 0.02	0.54 ± 0.03	0.33 ± 0.13	0.08	−0.16	0.50	0.20
b	0.63 ± 0.02	0.51 ± 0.03	0.31 ± 0.07	0.11	−0.16	0.49	0.25
c	0.73 ± 0.03	0.63 ± 0.01	0.49 ± 0.02	0.24	−0.04	0.62	0.52
d	0.84 ± 0.03	0.80 ± 0.01	0.76 ± 0.04	0.55	0.27	0.81	0.76

takes place within a fibre can be effectively eliminated by immersing the fibre in a liquid which has a similar refractive index to that of the fibre.

Acknowledgements

We should like to thank Mr C. H. Belford for his help in running the Raman spectra of the fibres and Mr G. Oglivy for supplying the fibres and the values of their birefringence. We are also grateful to the S.E.R.C. for the provision of a grant for spectroscopic studies of polymers.

References

1 Purvis, J., Bower, D. I. and Ward, I. M. *Polymer* 1973, **14**, 398
2 Purvis, J. and Bower, D. I. *Polymer* 1974, **15**, 645
3 Purvis, J. and Bower, D. I. *J. Polym. Sci., Polym. Phys. Edn.* 1976, **14**, 1461
4 Robinson, M. E. R., Bower, D. I. and Maddams, W. F. *J. Polym. Sci., Polym. Phys. Edn.* 1978, **16**, 2115
5 Jasse, B. and Koenig, J. L. *J. Polym. Sci., Polym. Phys. Edn.* 1980, **18**, 731
6 Jarvis, D. A., Hutchinson, I. J., Bower, D. I. and Ward, I. M. *Polymer* 1980, **21**, 41
7 Nobbs, J. H., Bower, D. I., Ward, I. M. and Patterson, D. *Polymer* 1974, **15**, 287
8 Bower, D. I. *J. Phys. B: Atom. Molec. Phys.* 1976, **9**, 3275
9 Daubeny, R. de P., Bunn, C. W. and Brown, C. J. *Proc. Roy. Soc. Lond.* 1955, **A226**, 531

A second comment on the histogram method in photon correlation spectroscopy applied in dilute polymer solutions

Erdogan Gulari
Chemical Engineering Department, University of Michigan, Ann Arbor, Michigan, 48104, *USA*

and Esin Gulari
Chemical Engineering Department, Wayne State University, Detroit, Michigan 48202, *USA*

and B. Chu
Chemistry Department, State University of New York at Stony Brook, Long Island, New York, 11794, *USA*

(*Received* 13 *November* 1981; *revised* 30 *December* 1981)

The histogram method approximates the linewidth distribution function and permits us to obtain an estimate of the molecular weight distribution function by making only one measurement of the time correlation function of a polymer solution of known molecular weight at one concentration and one scattering angle. Caroline has corrected a conceptual error on the collective coefficient $\bar{k}_D$. However, it is incorrect to assume that an incorrect estimate of k_D invalidates all our conclusions because the changes introduced by our erroneous computation of k_D is smaller than the difference predicted by the theoretical descriptions of Yamakawa, Imai and of Pyun and Fixman.

Keywords Analysis; histogram; photon correlation; polymer dispersity; molecular weight distribution

In a recent comment by Caroline[1] on our histogram method of data analysis for polystyrene in cyclohexane[2], he has correctly pointed out that for a polydisperse polymer in solution,

$$D(M) = D^0(M)(1 + \bar{k}_D{}^\theta C) \quad (1)$$

where $\bar{k}_D{}^\theta = -p\bar{v}_h - v$. p is unity in the theories of Yamakawa[3] and Imai[4] and 2.23 according to the 'soft-sphere' model of Pyun and Fixman[5]. v is the specific volume of the bulk polymer and $\bar{v}_h$ is the weight-average specific hydrodynamic volume as defined by

$$\bar{v}_h = \int f(M) M v_h \mathrm{d}M / \int f(M) M \mathrm{d}M \quad (2)$$

where $f(M)$ is the molecular weight distribution function. Since $D(M) = \Gamma/K^2$ and $D^0(M) = k_T M^{-1/2}$, we have

$$\Gamma/K^2 = k_T M^{-1/2}(1 + \bar{k}_D{}^\theta C) \quad (3)$$

As $\bar{k}_D{}^\theta$ varies with polymer polydispersity, it becomes necessary to determine $\bar{k}_D{}^\theta$ in order to transform $G(\Gamma)$ to $f(M)$ at finite concentrations. However, his statement that 'their conclusions may need revising' is not appropriate because we have actually used a fairly narrow molecular weight distribution polymer with maximum variation in molecular weight by a factor of about 2. The corresponding variation in $k_D{}^\theta$ is shown in *Table 1*. We see that the maximum deviation from the mean is $\pm 15\%$ with a standard deviation of $\sim 8\%$. Thus, irrespective of the exact $k_D{}^\theta$ values, our conclusions remain the same.

Caroline states that 'the best that could be achieved with the histogram method is to obtain a measure of $\bar{k}_D{}^\theta$ from a shift in the maximum of the histogram, but its

Table 1 $k^\theta_{D,i}$ values at C_1

$f(M) \times 10^5$ (arbitrary units)	$\Delta M_i \times 10^{-5}$	$M_i \times 10^{-5}$	$k^\theta_{D,i}$ (cm^3)
0.02	0.11	1.273	−23.6
0.87	0.11	1.385	−24.6
1.48	0.12	1.49	−25.6
1.51	0.15	1.63	−26.6
1.25	0.17	1.78	−27.9
0.79	0.21	1.98	−29.3
0.39	0.25	2.20	−30.9
0.01	0.30	2.48	−32.7

$\overline{k^\theta_D} = -27.7$ cm^3

0032-3861/82/050649-02$03.00